



## Effect of heat treatment on corrosion and electrochemical behaviour of AZ91D magnesium alloy

N.N. AUNG<sup>1</sup> and W. ZHOU<sup>2,\*</sup>

<sup>1</sup>School of Mechanical and Production Engineering, Nanyang Technological University, Singapore 639798;

<sup>2</sup>Division of Engineering and Applied Sciences, Harvard University, 9 Oxford Street, Cambridge, MA 02138-2901, USA

(\*author for correspondence, e-mail: wzhou@cantab.net)

Received 11 July 2001; accepted in revised form 28 August 2002

**Key words:** ageing, corrosion, heat treatment, magnesium alloy, precipitation

### Abstract

An AZ91D ingot in the as-cast condition was homogenized by solution treatment and then aged for various periods of time. The microstructures produced were studied in detail and the  $\beta$  phase volume fraction was measured quantitatively. The Corrosion resistance of all the different microstructures was studied in 3.5% NaCl solution through weight loss measurement in constant immersion conditions and potentiodynamic polarization experiments. The corroded surfaces were analysed using SEM and XRD. The volume fraction of the  $\beta$  phase was found to have a significant influence on the corrosion behaviour. The T4 condition improved the corrosion resistance of AZ91D alloy compared to the T6 heat treatment. The results support the idea of microgalvanic coupling between cathodic  $\beta$  phase and anodic  $\alpha$  matrix.

### 1. Introduction

Homogenization and subsequent ageing treatment of AZ91D alloy are known to offer considerable improvement in mechanical properties [1–3]. Early studies on ageing of magnesium alloys showed improved strength with increasing refinement of precipitates and the conditions for producing finer precipitates were lower ageing temperature, shorter ageing time and lower Al content [1, 2].

However, such heat treatment may have a great impact on corrosion behaviour due to the modification of microstructures. Ageing treatment of homogenized AZ91D alloy leads to the precipitation of  $\beta$  phase along the grain boundaries. The size and morphology of the precipitates depend on the ageing temperature, time and specific processing route. As  $\beta$  phase may act either as an effective cathode or a physical barrier to corrosion, depending on its volume fraction, it is important to study the influence of this phase on corrosion and electrochemical behaviour.

Clark [4] reported an age hardening mechanism in an AZ91 series magnesium alloy and found that both discontinuous and continuous  $\beta$  precipitation occurred during ageing. The discontinuous precipitation was made up of alternating lamellae of  $\beta$  phase and equilibrium composition matrix growing behind a migrating grain boundary. Crawley and Milliken [5] studied the ageing behaviour of AZ91 and found that

the orientation relationship of the continuous precipitation is consistent with that reported by Clark. Lunder [6] and Beldijoudi et al. [7] studied the relationship between the microstructure and the corrosion behaviour of AZ91 alloys in the solution-treated (T4) and 16 h artificially aged (T6) conditions. According to their work, ageing to T6 precipitates  $\beta$  phase, which improves the corrosion resistance.

Although several studies have been reported in relation to heat-treated microstructures and the effect of heat treatment on corrosion behaviour, the role of  $\beta$  volume fraction on corrosion and electrochemical behaviour is still not well understood. The present study aimed to examine the microstructures and corrosion behaviour of an AZ91D alloy under a wide range of conditions (as-cast, T4, and T6 with different ageing times) in order to understand the role of the  $\beta$  volume fraction on the corrosion and electrochemical behaviour in this important ultralight structural material.

### 2. Experimental procedures

#### 2.1. Material

An AZ91D ingot was used and it was sectioned to sample size of 10 mm  $\times$  10 mm  $\times$  2 mm for all the experiments. The Chemical composition of the alloy is given in Table 1.

Table 1. Chemical composition of the AZ91D alloy (in wt %)

Al	Mn	Ni	Cu	Zn	Ca	Si	K	Fe	Mg
9.1	0.17	0.001	0.001	0.64	<0.01	<0.01	<0.01	<0.001	Bal

## 2.2. Heat treatment

According to ASM standard the recommended solution-treating for AZ91 casting is 16–24 hr at 413 °C and ageing time is 16 h at 168 °C [8]. In this work homogenization heat treatment (T4) was performed at 420 °C for 24 h in argon atmosphere followed by water quench at 25 °C. The solution treated alloy was aged artificially (T6) in a vacuum oven at 200 °C for 8 h, 16 h, and 26 h, respectively, to produce microstructures of varying  $\beta$  volume fractions.

## 2.3. Corrosive medium

The 3.5% NaCl solution test medium was made with AR grade NaCl and distilled water. The pH value was measured to be 7.25. All corrosion tests were carried out at room temperature.

## 2.4. Constant immersion testing

The specimens were ground on progressively finer emery papers up to 1000 grade and then polished using 6  $\mu$ m diamond paste. All the specimens were initially cleaned following the procedure of ASTM standard G-I-72 [9]. The polished and preweighed specimens were exposed to 150 ml of 3.5% NaCl solution for a constant time. At the end of the experiment, final cleaning of the specimen was carried out by dipping it in a solution of 15% CrO<sub>3</sub> + 1% AgCrO<sub>4</sub> in 100 ml of boiling water. An acetone washing followed this. The weight loss was measured after each experiment and duplicate experiments were conducted. The corrosion rate in millimetre per year (mm y<sup>-1</sup>) was calculated using the weight loss measurements.

## 2.5. Electrochemical testing

Electrochemical polarization experiments were carried out using a potentiostat/galvanostat model 263A corrosion measurement system. Electrodes for this study were prepared by connecting a wire to one side of the sample that was covered with cold setting resin. The opposite surface of the specimen was exposed to the solution. The exposed area was about 1 cm<sup>2</sup>. The specimens were given a metallographic polish prior to each experiment, followed by washing with distilled water and acetone. Polarization measurements were carried out in a corrosion cell containing 150 ml of 3.5% NaCl solution using a standard three-electrode configuration: saturated calomel as a reference with a platinum electrode as counter and the sample as the working electrode. Specimens were immersed in the 3.5% NaCl

solution. A polarisation scan was carried out towards more noble values at a rate of 1 mV s<sup>-1</sup>, after allowing a steady state potential to develop.

## 2.6. Surface morphology

The microstructure and surface morphology of the corroded surfaces were characterized using optical microscopy (Zeiss model) and scanning electron microscopy (SEM, Jeol model 5600LV) coupled with energy dispersed spectroscopy (EDS) system to identify the  $\beta$  phase. An image analyser (Image-Pro Plus) software was used to capture the images and calculate the percentage covered by the  $\beta$  phase on as-polished samples. X-ray diffraction (XRD, Philips, model PW1830) was performed on the bulk specimens to confirm the new secondary phases.

## 3. Results and discussion

### 3.1. Effect of heat treatment on microstructures

The microstructure of the ingot in the as-cast condition was observed to contain primary  $\alpha$ , eutectic  $\alpha$ , and  $\beta$  precipitates, as reported earlier [3, 10]. The homogenization heat treatment at 420 °C for 24 h was found to be effective in dissolving the  $\beta$  precipitates in the as-cast ingot, as shown in Figure 1(a). Artificial ageing causes precipitation of the  $\beta$  phase, as shown in Figure 1(b)–(d). For the 8 h ageing,  $\beta$  particles precipitated mainly along grain boundaries (Figure 1(b)). When the ageing time was increased to 16 h and 26 h,  $\beta$  phase was found to increase in amounts and grow through the grain discontinuously, as can be seen in Figure 1(c) and (d). The longer the ageing time the larger the amount of  $\beta$  volume fraction observed, and this trend is shown more clearly in Figure 2. It should be mentioned that the quantitative image analysis of the  $\beta$  volume fraction was carried out under the SEM, since some  $\beta$  precipitates are too fine to be resolvable by light microscopy [11].

### 3.2. Effect of ageing on corrosion rates

The corrosion behaviour of the heat treated AZ91D alloy depends on how the microconstituents interact with the aqueous environments to which they are exposed. In the current study, the variation of corrosion rate as a function of ageing time after exposure for a period of 8 h was studied. As shown in Table 2, homogenization of the as-cast ingot leads to the best corrosion resistance, but the corrosion rate became higher after the microstructure was aged for 8 h, 16 h or 26 h.

The deterioration of corrosion resistance in the aged microstructures is related to the  $\beta$  phase. The  $\beta$  phase is known to play a dual role in corrosion processes of magnesium alloys [12, 14]. On the one hand,  $\beta$  phase itself has a high resistance to corrosion, so it may play

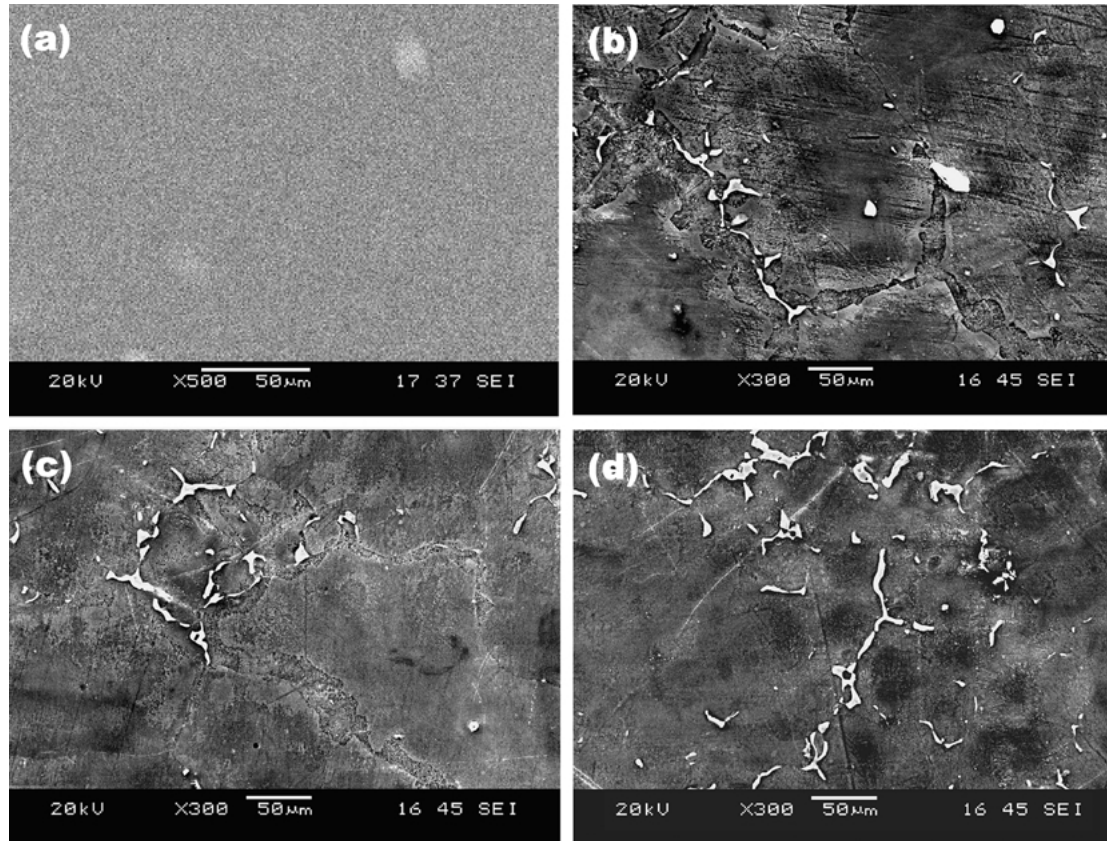


Fig. 1. Scanning electron micrographs showing the effect of ageing time on precipitation of  $\beta$  phase along the grain boundaries of AZ91D ingot alloy (a) homogenization, (b) ageing for 8 h, (c) ageing for 16 h and (d) ageing for 26 h. Magnifications: (a)  $\times 500$ , (b)  $\times 300$ , (c)  $\times 300$  and (d)  $\times 300$ .

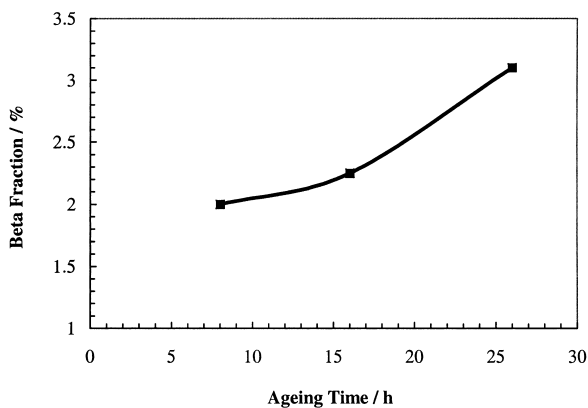


Fig. 2. Effect of ageing time on the amount of precipitated  $\beta$  phase.

Table 2. Effect of heat treatment on corrosion rate of AZ91D ingot

Heat treatment	Corrosion rate/mm $y^{-1}$
As-Cast	4.0
Homogenization	1.6
8 h ageing	3.2
16 h ageing	2.5
26 h ageing	2.8

the role of reducing corrosion rate by forming a barrier of  $\beta$  once the less noble phase is dissolved [5, 6, 13]. On the other hand,  $\beta$  phase is highly cathodic to the matrix

and can thus act as an effective cathode to cause galvanic corrosion in anodic  $\alpha$  matrix [12]. The observation of poorer corrosion resistance in the aged microstructures indicates that  $\beta$  acted as cathode to cause galvanic corrosion.

According to our previous study [12], the size and morphology of  $\beta$  phase have significant influence on corrosion behaviour of AZ91D alloy and corrosion is usually initiated in regions containing less than 8% aluminium. Therefore, the aluminium content of the AZ91D matrix is another important factor that must be considered. Higher corrosion rate in aged conditions appeared to be influenced by the  $\beta$  phase in relation to lower aluminium content in the matrix. A lower amount of cathodic  $\beta$  phase and homogeneity of higher aluminium content matrix in T4 alloy prevented severe corrosion attack and the result therefore showed the best corrosion resistance for T4 condition.

The above results were confirmed by SEM micrographs for the different corroded surfaces of AZ91D ingot in the T4 and T6 conditions, as shown in Figure 3. The T4 condition exhibited a few deep pits distributed uniformly on the surface (Figure 3(a)). For the same alloys in the 8 h, 16 h and 26 h ageing conditions, localized attack zones were found to be more severe than with T4 condition (Figure 3(b)–(d)). The attack was found to increase with increasing ageing time (i.e., increasing  $\beta$  volume fraction).

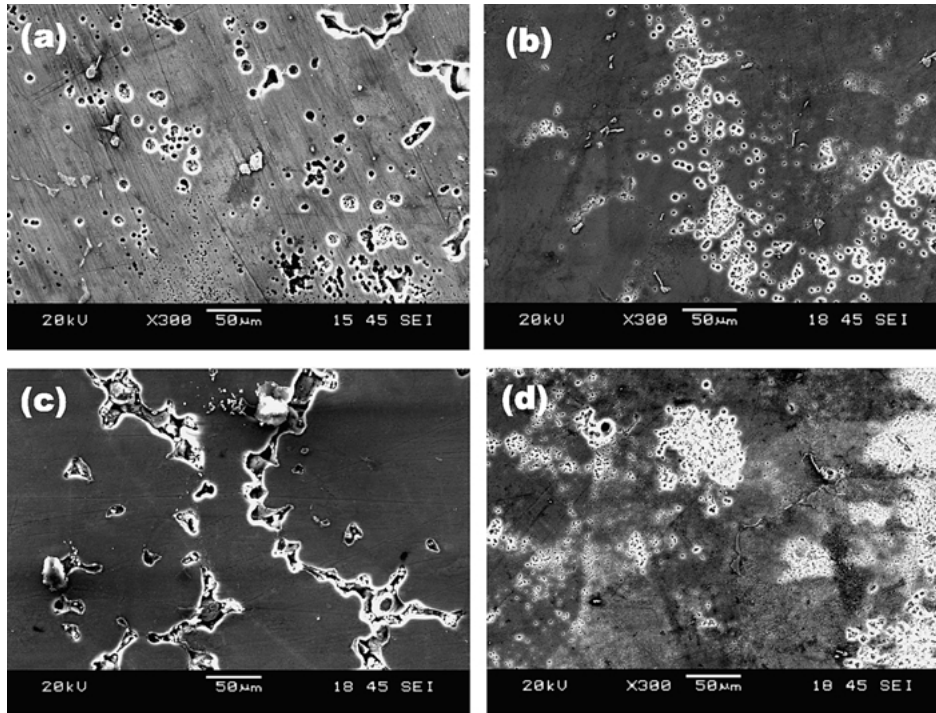


Fig. 3. Scanning electron micrographs showing the corroded surfaces of AZ91D ingot at different ageing time after (a) homogenization, (b) ageing for 8 h, (c) ageing for 16 h and (d) ageing for 26 h. Magnifications: (a)–(d)  $\times 300$ .

A  $\rightarrow$  Mg, B  $\rightarrow$   $\beta$ , C  $\rightarrow$  MgO:Al<sub>2</sub>O<sub>3</sub>

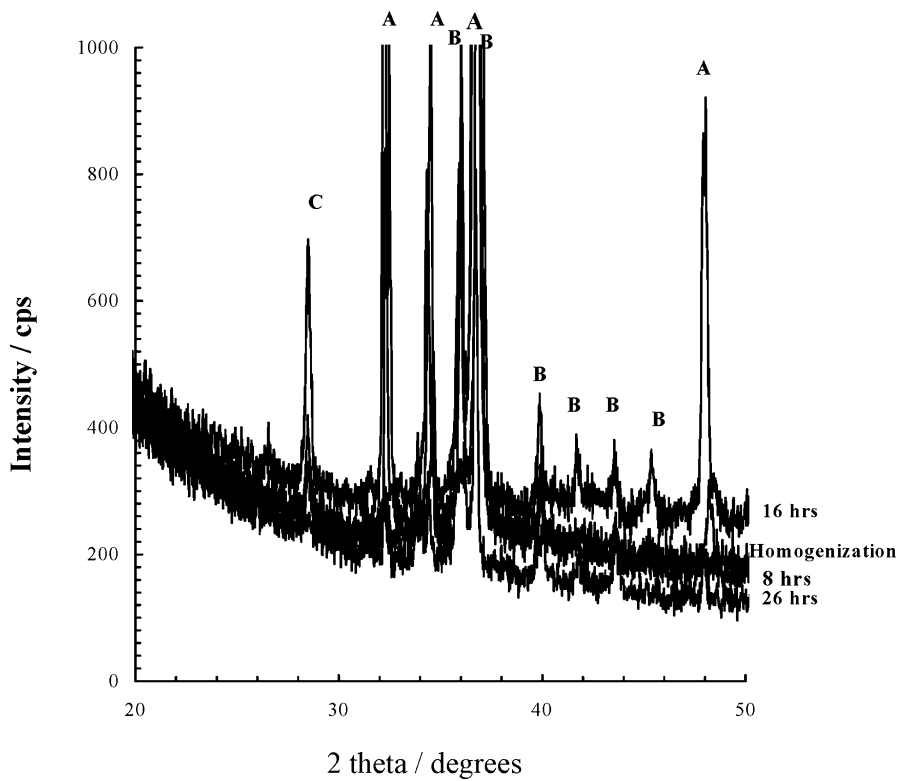


Fig. 4. XRD patterns of AZ91D surfaces in various conditions after exposure to 3.5% NaCl solution for 48 h.

3.3. Corrosion product

XRD patterns were taken on specimens tested under constant immersion for 48 h, as shown in Figure 4. The

Figure shows the intensities of the peaks corresponding to Mg,  $\beta$  phase and MgO  $\cdot$  Al<sub>2</sub>O<sub>3</sub>. The study confirms that corrosion products of the heat treated AZ91D microstructures contain mixed magnesium–aluminium

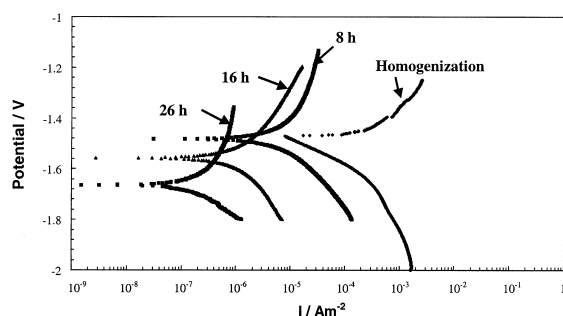


Fig. 5. Potentiodynamic polarization curves for T4 and T6 AZ91D ingot at different ageing times in 3.5% NaCl solution.

oxides, as do the corrosion products of the as-cast AZ91D ingot [10].

### 3.4. Effect of heat treatment on electrochemical behaviour

The electrochemical behaviour of the T6 AZ91D ingot at different ageing times was investigated by comparing with that of the homogenized microstructure (T4). The potentiodynamic polarization curves of these microstructures in 3.5% NaCl solution are shown in Figure 5. No microstructures showed any passivity in this solution.

Table 3 shows the  $E_{\text{corr}}$ , Tafel slope and  $I_{\text{corr}}$  values for all the microstructures. The Tafel slope is similar for all the three ageing times, indicating similar electrochemical reactions in the aged microstructures. The overpotential for the cathodic reaction was lower on T6 specimens than on T4. It is interesting to note that  $I_{\text{corr}}$  for the 26 h ageing specimen is very low (Table 3) though the corrosion rate for the aged microstructures are higher than for the T4 condition (Table 2). The decrease of  $I_{\text{corr}}$  value for the T6 condition is thought to be due to the larger  $\beta$  volume fraction. In the electrochemical behaviour of the T6 condition it has been generally agreed that the larger volume fraction of  $\beta$  phase is beneficial in improving the corrosion behaviour of magnesium alloys because the  $\beta$  phase along the grain boundary acts as a physical barrier to corrosion [5, 6, 13].

The main reason for the discrepancy between the electrochemical behaviour and weight loss corrosion rate is that the inhibiting effect of the  $\beta$  phase in the T6 alloy predominated during short interval of electrochemical testing but the accelerating effect of the decrease in Al content in the matrix predominated in the long period immersion testing. Another point to note is that  $\beta$  phase particles might break away from the

Table 3.  $I_{\text{corr}}$ ,  $E_{\text{corr}}$  and  $\beta_c$  values for T4 and T6 AZ91D ingot in 3.5% NaCl solution

Material	$I_{\text{corr}}/\text{mA cm}^{-2}$	$E_{\text{corr}}/\text{V}$	$\beta_c/\text{mV}$
Homogenization	0.8	-1.55	181
8 h ageing	0.05	-1.50	411
16 h ageing	0.085	-1.56	480
26 h ageing	0.0015	-1.66	360

matrix during the long period of immersion testing and fall into the chemical solution [10, 12, 14] and this also tends to increase the corrosion rate of the T6 specimens.

## 4. Conclusions

- (i) Homogenization treatment of an AZ91D ingot at 420 °C for 24 h was found to be effective in dissolving the  $\beta$  precipitates. Artificial ageing at 200 °C caused precipitation of  $\beta$  phase mainly along the grain boundaries. The volume fraction of  $\beta$  phase was observed to increase with ageing time.
- (ii) Homogenization treatment improves corrosion resistance of the AZ91D ingot, but ageing of the microstructure for 8 h, 16 h or 26 h lowers corrosion resistance. The results support the suggestion that there exists microgalvanic coupling between cathodic  $\beta$  phase and anodic  $\alpha$  matrix. The XRD study indicates the presence of mixed magnesium–aluminium oxides in the corrosion products of the heat treated AZ91D microstructures.
- (iii) The volume fraction of the  $\beta$  phase was observed to affect the corrosion behaviour of AZ91D alloy. The inhibiting effect of the  $\beta$  phase in the artificially aged alloy predominated during the short interval of electrochemical testing but the accelerating effect of the decrease in aluminium content in the matrix predominated in the long period immersion testing. During immersion testing,  $\beta$  phase may fall into the chemical solution and this also tends to accelerate the corrosion rate.

## References

1. F.A. Fox and E. Lardner, *J. Inst. Met.* **49** (1943) 373.
2. T.E. Leontis and C.E. Nelson, *Trans. AIME* **191** (1951) 120.
3. A. Bag and W. Zhou, *J. Mater. Sci. Lett.* **20** (2001) 457.
4. J.B. Clark, Age Hardening in a Mg-9wt.% Al alloy, *Acta Metall.* **16** (1968) 141.
5. A.F. Crawley and K.S. Milliken, Precipitate Morphology and Orientation Relationship in an Aged Mg-9% Al-1% Zn-0.3% Mn Alloys, *Acta Metall.* **22** (1974) 557.
6. O. Lunder, J.E. Lein, T.Kr. Aune and K. Nisancioglu, *Corrosion* **45** (1989) 741.
7. T. Beldijoudi, C. Fiaud and L. Robbiola, *Corrosion* **8** (1993) 738.
8. M.M. Avedesian and H. Baker, 'Magnesium and Magnesium Alloys', ASM Speciality Handbook (1999), p. 78.
9. Annual Book of ASTM Standards Parts 3 and 4 (1977), p. 722.
10. R. Ambat, N.N. Aung and W. Zhou, *J. Appl. Electrochem.* **30** (2000) 865.
11. A.A. Kaya, P. Uzan, D. Eliezer and E. Aghion, *Mater. Sci. Technol.* **16** (2000) 1001.
12. R. Ambat, N.N. Aung and W. Zhou, *Corros. Sci.* **42** (2000) 1433.
13. P. Uzan, N. Frumin, D. Eliezer and E. Aghion, The Role of Composition and Second Phases on the Corrosion Behaviour of AZ Alloys, in E. Aghion and D. Eliezer (Eds), Proceedings of the 2nd Israeli International Conference on 'Magnesium Science and Technology', Magnesium 2000, Dead Sea, Israel (Feb. 2000), p. 285.
14. S. Mathieu, C. Rapin, J. Hazan and P. Steinmetz, *Corro. Sci.* **44** (2002) 2737.